

## EXPERIMENTAL INVESTIGATION OF FLAME STABILIZATION IN COAXIAL LOX/H<sub>2</sub> AND LOX/CH<sub>4</sub> SPRAY FLAMES

M. Oschwald\*, S. Naclerio\*, B. Yang<sup>o</sup>, F. Cuoco<sup>#</sup>

\*German Aerospace Center (DLR), Institute of Space Propulsion, Lampoldshausen, Germany

Telefon: +49 6298 28 327, Fax: +49 6298 28 175, email: michael.oschwald@dlr.de

<sup>o</sup>Northwestern Polytechnique University, Xi'an, China

### ABSTRACT

Results are presented from experimental investigations of reactive coaxial LOX/H<sub>2</sub> and LOX/CH<sub>4</sub>-spray flames. Spray and flame phenomenology have been evaluated for various injection conditions and the effect of Weber-number  $We$  and momentum flux ratio  $J$  has been analyzed. LOX/H<sub>2</sub> and LOX/CH<sub>4</sub>-spray flames show similar trends as function of  $We$  and  $J$ , however when comparing the spray flames at similar injection conditions the significant effect of the type of fuel is observed. For LOX/H<sub>2</sub>-flames visualization data obtained in a pressure range from near ambient to supercritical pressures for oxygen at the test facilities M3.1 and P8 test benches confirm the stabilization of the combustion zone in the small recirculation zone at the injector exit. However in experiments with LOX/CH<sub>4</sub> at chamber pressures near 0.15MPa at M3.1 lifted flames are observed for rather all operating conditions. The analysis of the lifted flames clearly shows the interaction of the combustion process with the liquid jet atomization. For momentum flux ratios  $J < 0.3$  a linear dependence of the lift-off distance from the  $We$ -number has been found.

### INTRODUCTION

There is increased interest in hydrocarbons as fuel for rocket propulsion. The main advantages of using hydrocarbons are their high propellant density, the reduced handling effort, and reduced safety precautions as compared to liquid hydrogen or hypergolic propellants. Among the hydrocarbons methane and kerosene are of particular interest. We have chosen methane as a candidate propellant and as the simplest representative for a hydrocarbon fuel to investigate various aspects related to rocket combustor technology, regenerative cooling [1], kinetics of LOX/CH<sub>4</sub> [2], propellant injection [3] and ignition [4].

Propellant injection is a key technology for optimum rocket combustor performance due to its effect on liquid fuel atomization, mixing, combustion, and thermal and chemical loads on the combustor walls. Propellant injectors are controlling by a major part efficiency and stability of combustion. In main combustion chambers oxygen is injected in its liquid state, whereas the fuel - used for regenerative cooling the combustor walls - is injected in the gaseous state. The standard injection element is the shear co-axial injector with the liquid injected through the central tube and the gaseous fuel through the annular slit. For the gas flow the downstream end of the LOX post forms a step of finite height over the surface of the liquid oxygen jet. It has been consistently observed that LOX/H<sub>2</sub> spray flames stabilize in the wake of the flow behind this step.

The complexity of the atomization process today does not allow a prediction of spray properties derived from basic principles and the design of injectors is mainly based on empirical rules. Numerous experimental and theoretical investigations have been done on coaxial injection of non-reactive flows to improve the understanding of the

atomization process [5]-[17]. Prominent non-dimensional numbers found as parameters controlling the injector performance are the Weber number  $We$

$$We = \frac{\rho_g (u_g - u_l)^2 d_l}{\sigma}$$

and the momentum flux ratio  $J$

$$J = \frac{(\rho u^2)_g}{(\rho u^2)_l}$$

where  $d_l$  is the inner diameter of the LOX post and properties of gas and liquid are labelled with the indices  $g$  and  $l$  respectively. A typical value for the injection of LOX/H<sub>2</sub> in rocket combustors is a momentum flux ratio of  $J \sim 10$ . In cold flow tests  $J$  has been found to determine the liquid intact core length  $L$  in coaxial injection [12]-[14] and a functional dependence of the form

$$\frac{L}{d_l} = \frac{a}{J^n} \quad (1)$$

has been found. For a two phase coaxial jet Davis [13] determined the parameters  $a=25$  and  $n=0.2$ .

In reactive sprays however there is a notable interaction of combustion and atomization. In Figure 1 a LOX/H<sub>2</sub> spray flame is visualized by backlight imaging and recording the chemiluminescence of the OH-radical. The flame is seen to be anchored at the LOX post and it is located between the LOX jet and the annular H<sub>2</sub> flow. It is clear that the atomization process is thus not only controlled by the aerodynamic forces between the two fluids and the surface tension of the liquid. Heat release and the reaction products from the combustion process introduced into the turbulent shear layer between the oxygen core flow and the annular fuel flow are changing the

conditions for atomization and droplet vaporization. The propellant atomization, mixing and combustion process therefore can't be only controlled by the propellant injection conditions as expressed by  $We$ -number and momentum flux ratio. As will be shown below the type of propellant, in our investigation either hydrogen or methane, has an influence on characteristic LOX spray properties like LOX intact core length under hot fire conditions. Also flame characteristics like flame anchoring mechanism show different behaviour for different types of fuel. Using numerical simulation Juniper and Candel [18] investigated the flame anchoring process of a diffusion flame at a step of height  $h_s$  over a liquid reactant. In their work they identified the non-dimensional group

$$\Psi = \frac{h_s}{\delta_f}, \quad (2)$$

the ratio between step height and flame thickness

$$\delta_f = 1/\sqrt{\tau_c \mathcal{D}}, \quad (3)$$

to be the most effective parameter regarding flame stabilization. For our problem the step height  $h_s$  can be identified with the thickness of the LOX post.  $\tau_c$  and  $\mathcal{D}$  are the chemical time scale and the species diffusivity respectively. The numerical results obtained in [18] predict flames attached to the step for values of  $\Psi > 1$  and unstable solutions for  $\Psi < 0$ . As discussed below for the LOX/CH<sub>4</sub> case rather always lifted flames have been observed in the experiments presented here whereas for the LOX/H<sub>2</sub> case flames have been always found to be attached to the LOX-post. The non-dimensional group  $\Psi$  will be discussed below in view of these experimental results.

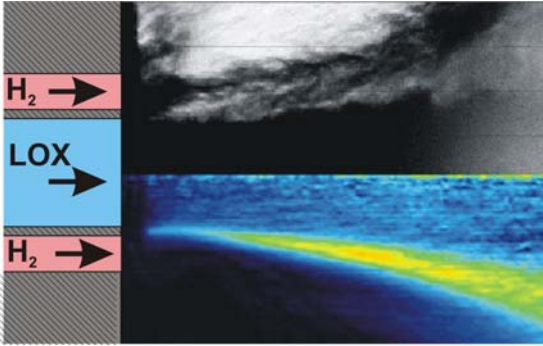


Figure 1: Backlight imaging (top) and OH imaging (bottom) of a burning LOX/H<sub>2</sub> spray in combustor C at the P8 test bench [19]

## EXPERIMENTAL SETUP

### M3.1 Test bench and micro combustor

The M3.1 test bench is small scale facility for experimental investigations of combustion processes using liquid oxygen as oxidizer and hydrogen or hydrocarbons as fuels. Propellants can be supplied at cryogenic or ambient temperatures.

The micro combustor has a squared cross section of 6cm x 6cm (see Figure 2). Quartz windows allow optical access to the full combustor volume. Combustion chamber pressure during steady state combustion in the tests was 0.15MPa. The combustor is capacitively cooled, the run time is thus limited to about 2s.

Propellants have been injected into the combustion chamber by a coaxial injection element. Two different LOX

posts have been used with thicknesses  $h_s = 0.4\text{mm}$  and  $0.6\text{mm}$ . The injector design also allowed the variation of the annular slit width from 4.8mm to 6.9mm and thus the variation of injection exit velocities at mixture ratios  $R_{OF} = 5.5$  and  $3.4$  for LOX/H<sub>2</sub> and LOX/CH<sub>4</sub> respectively. The ranges of Weber- and  $J$ -numbers achieved were between 500-20,000 and 0.1-2 respectively. As the interest was to identify the specific effects of  $We$  and  $J$  the definition of the test matrix was aiming to vary both parameters independently and to span a maximum area in the  $We/J$ -plane. The test conditions that have been realized within our experimental constraints are shown in Figure 3.

Tests have been done with LOX and the fuels hydrogen at 80K or methane at ambient temperature. Thermo-physical properties of the propellants are listed in Table 1.

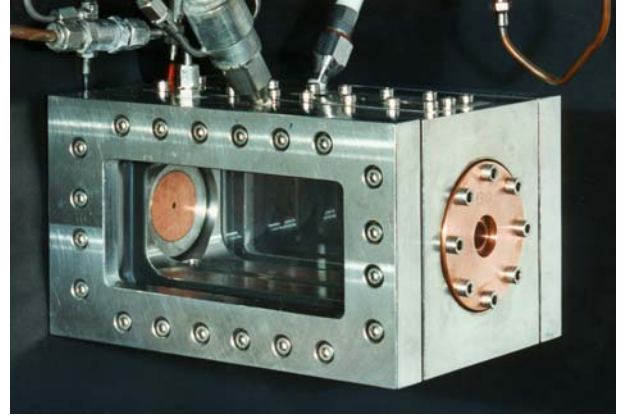


Figure 2: Micro Combustor.

	CH <sub>4</sub>	H <sub>2</sub>
critical temperature $T_{crit}$ , K	190.5	32.9
critical pressure $p_{crit}$ , MPa	4.60	1.28
reduced pressure, $p/p_{crit}$	0.033	0.12
reduced temperature $T/T_{crit}$	1.51	2.43
density, $\text{kg/m}^3$	1.01	0.456
viscosity, $\mu\text{Pa}\cdot\text{s}$	10.86	3.57
specific heat, $\text{J/kg}\cdot\text{K}$	2,213	10,766
thermal conductivity, $\text{W/m}\cdot\text{K}$	0.0329	0.0566
thermal diffusivity, $10^{-5}\text{m}^2/\text{s}$	1.47	1.15
laminar flame velocity @ ambient, m/s	3.93	10.7
ignitability limits, Vol %	5.1-61	4-94

Table 1: Thermo-physical properties of propellants at injector exit conditions of this paper:  $p_C = 0.15\text{MPa}$ ,  $T = 80\text{K}$  for LOX and H<sub>2</sub>, ambient temperature for CH<sub>4</sub>

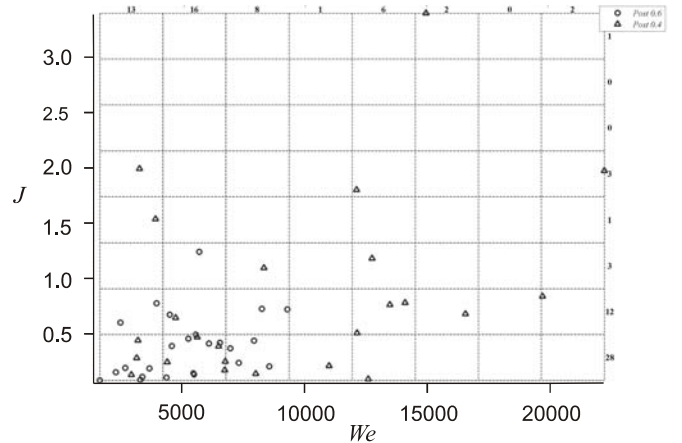


Figure 3: Test matrix in terms of momentum flux ratio  $J$  and Weber number.

## Visualization of flow and flame

Spray characteristics have been recorded by backlight imaging with a Kodak Flowmaster 2k camera. A nanolite with 18ns flash duration was used as light source.

The flame front was visualized with an intensified high-speed CCD camera with a 9 kHz acquisition rate and a 256×128pixel resolution. The camera was fitted with a UV lens and a narrow band filter (300-310nm) to record the OH radical emission during the combustion process.

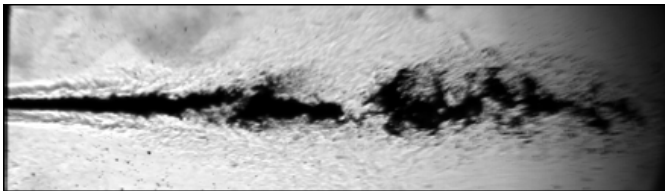
## RESULTS

### Comparison of LOX/H<sub>2</sub> and LOX/CH<sub>4</sub> spray flames

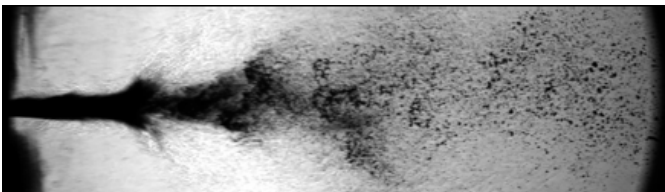
The role of momentum flux ratio and Weber number on atomization at hot fire conditions has been analyzed for LOX/H<sub>2</sub> and LOX/CH<sub>4</sub> in previous work [3] and the main results are summarized here.

The effect of momentum flux ratio  $J$  promotes jet instability and results in an earlier onset of jet disintegration. Increasing Weber number has been shown to promote disintegration into smaller ligaments and droplets at smaller distances downstream from the injector. Both trends have identically been observed for hydrogen and methane.

However when comparing LOX/H<sub>2</sub> sprays and LOX/CH<sub>4</sub> sprays at similar injection conditions in terms of  $J$  and  $We$  significant differences can be observed. Examples are shown in Figure 4 for  $We \sim 9850$  and about similar momentum flux ratios  $J=1.3$  and  $J=1.6$  for LOX/H<sub>2</sub> and LOX/CH<sub>4</sub> respectively. For LOX/CH<sub>4</sub> the intact liquid core length of the LOX jet is shorter, the liquid is atomized in much finer droplets, and the droplets are spread in a much larger volume than in the case of LOX/H<sub>2</sub>. This difference in spray phenomenology at similar injection conditions is observed consistently at all investigated test conditions.



(a) LOX/H<sub>2</sub>:  $We=9844$ ,  $J=1.28$



(b) LOX/CH<sub>4</sub>:  $We=9885$ ,  $J=1.62$

Figure 4: Comparison of reactive (a) LOX/H<sub>2</sub> and (b) LOX/CH<sub>4</sub> sprays at similar injection conditions.

The most significant difference observed was however that for LOX/CH<sub>4</sub> detached flames have been observed for rather all injection conditions in these tests. Whereas for LOX/H<sub>2</sub> the flame was always anchored at the LOX post, for rather all injection conditions at  $p_c=0.15\text{MPa}$  for methane the spray flame stabilized at some distance downstream the injector in the mixing layer between the core oxygen and annular

methane flows. An example is given in Figure 5 where spray and flame visualizations for both propellant pairs are shown at similar injection conditions in terms of  $We$  and  $J$ . It is clearly seen that for methane the flame is anchored at a detached position. Correspondingly in the spray image a sudden change in the atomization behaviour at the flame anchoring position is observed. Droplets seem to experience a sudden increase in their radial velocity component and spray disintegration appears to be more violent downstream the anchoring position.

Depending on the flame anchoring mechanism distinctive different flame spreading angles are observed. Data on flame spreading angles for LOX/CH<sub>4</sub> and LOX/H<sub>2</sub> flames are shown in Figure 6. All LOX/H<sub>2</sub> flames investigated were anchored whereas rather all LOX/CH<sub>4</sub> flames were lifted off. Only in a small number of tests attached LOX/CH<sub>4</sub> flames were observed. Spreading angles are seen to be well correlated with the Weber number for both propellants. For the attached flames the spreading angles for hydrogen and methane are of similar size. The lifted methane flames show about 4 times larger spreading angles than the attached ones.

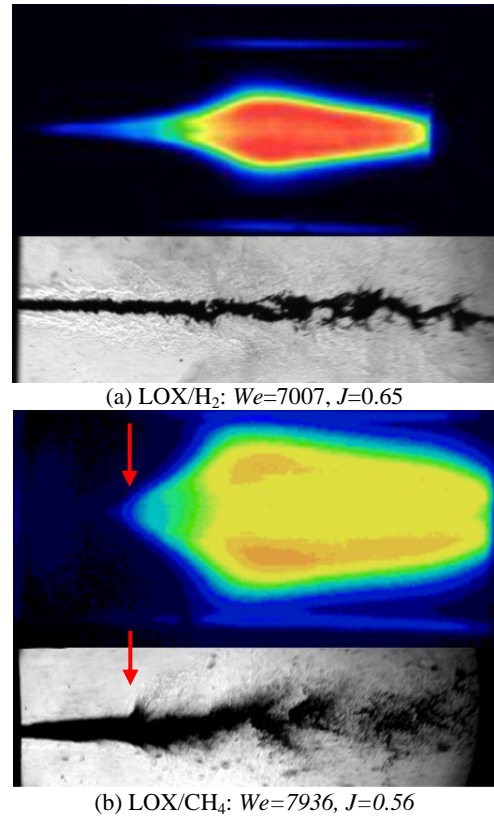


Figure 5: Comparison of reactive (a) LOX/H<sub>2</sub> and (b) LOX/CH<sub>4</sub> sprays and flames at similar injection conditions ( $P_c=1.5\text{ba}$ )

These observed features would be in agreement with following basic flame anchoring scenario sketched in Figure 7. Due to the shear forces between the gaseous annular and liquid core flow the LOX jet is beginning to disintegrate into droplets immediately downstream the injector exit. In the spray image of Figure 5b correspondingly the LOX jet diameter is seen slightly increasing downstream the injector exit with its boundary blurred due to the dense cloud of tiny droplets around the core flow. As at the injector exit evaporation of LOX droplets is just beginning the gas phase is mainly composed of the injected methane. On the way downstream droplet production is increasing and subsequent evaporation increases the available gaseous oxygen. By

turbulent and diffusive mixing premixed combustible gas is produced with increasing equivalence ratio downstream from the injector. The local burning velocity in the combustible gas is therefore increasing until at some distance from the injector it is able to balance the velocity of the convective flow. At this location the flame is anchored. Downstream the flame front the reaction products expand and this gives rise to the sudden increase of the radial movement of the droplets marked by the red arrow at the flame anchoring point in Figure 5b.

For the LOX/CH<sub>4</sub> spray flame the lift-off behaviour as function of the injection conditions will be addressed below in more detail. As the LOX post thickness is assumed to have a key influence on the flame stabilization behaviour first some results on the spray properties for LOX posts of different thickness are presented.

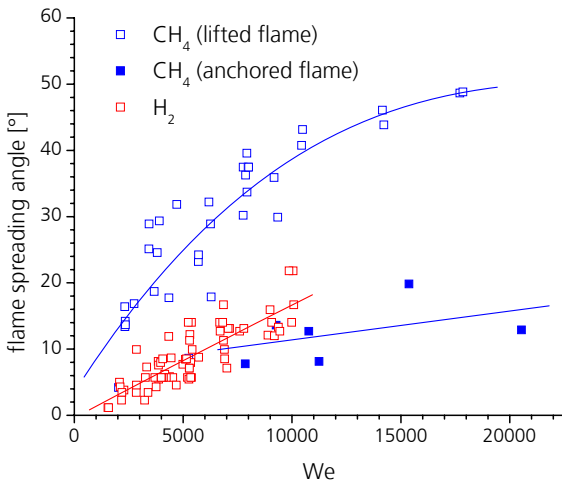


Figure 6: Flame spreading angle for LOX/CH<sub>4</sub>- and LOX/H<sub>2</sub>-spray flames as function of (a) Weber-number

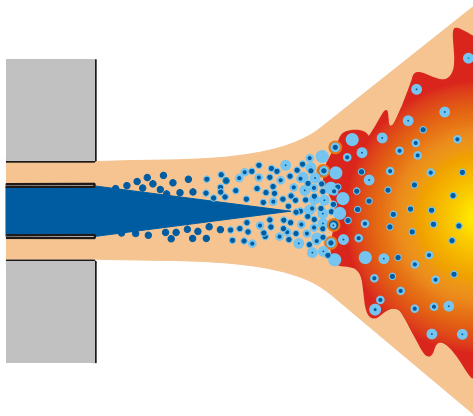


Figure 7: Sketch of atomization, evaporation and mixing for detached flame anchoring

#### Variation of the LOX-post thickness for LOX/CH<sub>4</sub>

The liquid intact core length for the burning LOX/CH<sub>4</sub> spray has been determined for LOX posts of thickness  $h_s=0.4\text{mm}$  and  $0.6\text{mm}$  and the data are shown in Figure 8. For both values of  $h_s$  a functional dependence according to equation (1) has been fitted resulting in  $a=24$  and  $n=0.34$  for  $h_s=0.6\text{mm}$  and  $a=18$  and  $n=0.24$  for  $h_s=0.4\text{mm}$ . Apparently for smaller LOX posts a longer liquid intact core length is observed. However, the data set is limited and there is lack of data at high  $J$ -values. Furthermore the momentum flux ratio  $J$

could not be adjusted independently from other parameters and other dependencies may be hidden in the data set.

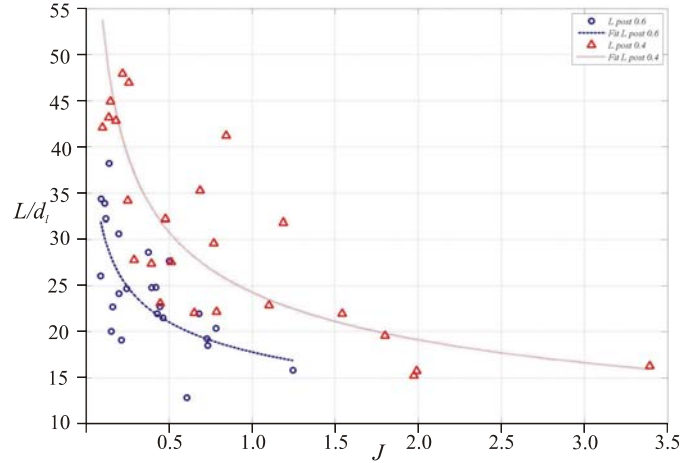


Figure 8: Intact core length of LOX/CH<sub>4</sub>-spray flame as function of momentum flux ratio  $J$  for LOX post thickness  $h_s=0.6\text{mm}$  (red) and  $h_s=0.4\text{mm}$  (blue)

In order to investigate a potential dependence on the Weber number all test with  $J<1$  are analyzed in two groups, the first group includes all tests with smaller  $We$ -numbers ( $1526<We<4124$ ), the second group all tests with higher  $We$ -numbers ( $4124<We<6723$ ). As can be seen in Figure 9 even with some scattering an influence of  $We$  on the intact core length for very small  $J$  values can be observed. For higher  $J$  values the influence of  $We$  seems to be less significant.

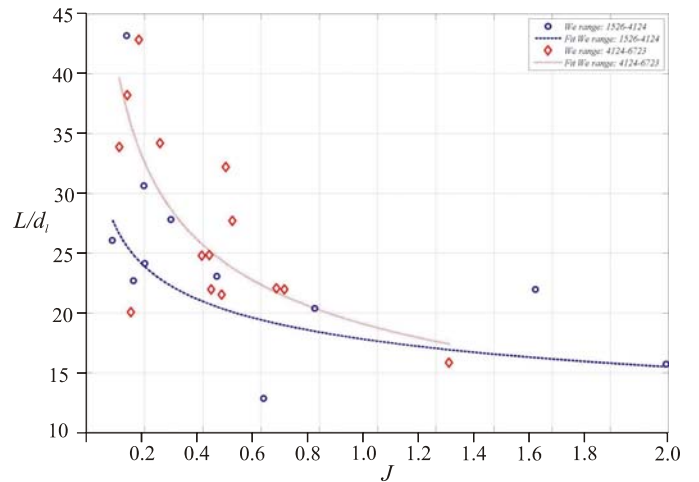


Figure 9: Intact core length of burning LOX/CH<sub>4</sub>-spray as function of  $J$  grouped for  $1526<We<4124$  (blue) and  $4124<We<6723$  (red).

For the subset of data with  $J<0.3$  the liquid intact core lengths are shown in Figure 10 as a function of  $We$ . At these small  $J$ -values the effect of the  $We$ -number on the intact core length can be well seen. With the exception of four tests all data are well grouping along a line given by  $L/d_i=We^{0.42}$ . It has to be noted that data points for both LOX post thicknesses are grouping similarly along the fitted line. A closer examination of the 4 outliers test shows that they had a specific flame phenomenology. Test E1 which has a longer  $L/d_i$  as other tests at similar  $We$  had been performed at an exceptional small equivalence ratio  $\Phi=0.68$ , the flame was attached to the injector and exhibits a very low level of OH chemiluminescence as compared to the other tests. Tests E2, E3, and E4 show a very intense flame as compared to the

other tests. The reason for the deviations of these tests from the other members of the set is not resolved and this is an indication that there are other control parameters contributing to the flame phenomenology.

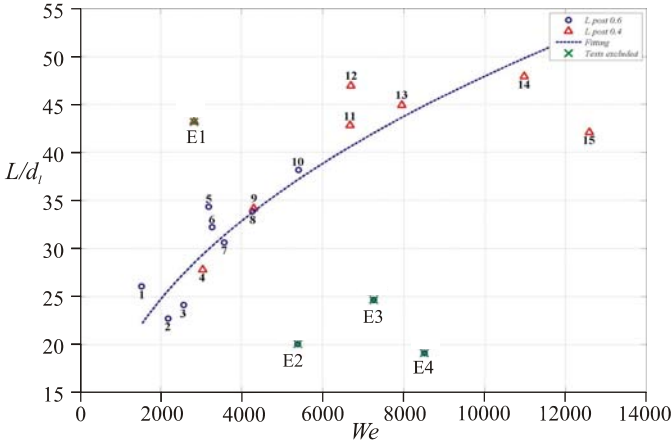


Figure 10: Intact core length LOX/CH<sub>4</sub>-spray flame as function of We-number for tests with  $J < 0.3$ .

### Flame lift-off for LOX/CH<sub>4</sub>-flames

Rather all tests with small momentum flux ratio ( $J < 0.3$ ) showed flame stabilization with detached flames. For these tests the distance of the flame anchoring position from the injector exit has been evaluated. The only significant correlation found between the lift-off distance and the injection conditions is a dependency from the Weber number. To illustrate the dependency visualizations of the flame and the spray have been overlaid and they are shown below in Figure 11 to Figure 13. With increasing Weber number an increase of the lift-off distance is observed. The plot of the lift-off distance as a function of  $We$  shown in Figure 14 resolves that the dependency is linear. Even the outlier tests showing specific behaviour with respect to the intact core length are well grouping near the trend line.

An extended analysis for all tests including tests with  $J > 0.3$  confirms the  $We$ -dependence, but that the lift-off distance is also influenced by the momentum flux ratio. The effect of  $J$  is opposite to  $We$ , increasing  $J$  is promoting shorter lift-off distances. The effect of  $J$  on the flame lift-off distance is coherent with the observation that increased  $J$  results in an earlier onset of jet disintegration.

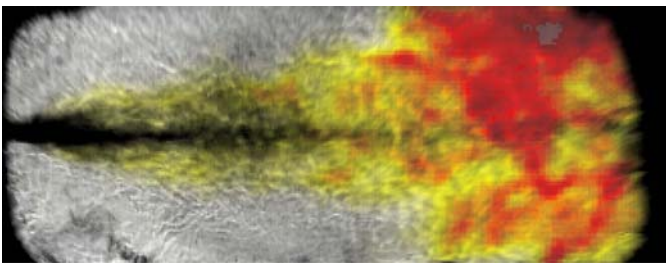


Figure 11: LOX/CH<sub>4</sub> spray and flame visualization for  $We=1526$ ,  $J=0.088$ .

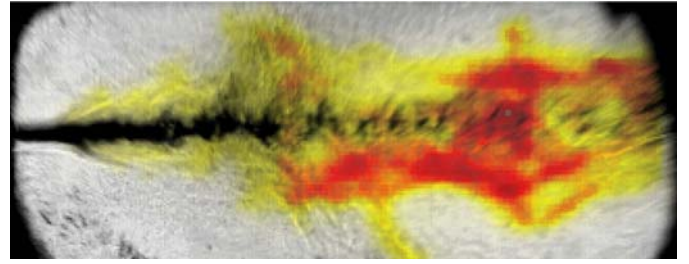


Figure 12: LOX/CH<sub>4</sub> spray and flame visualization for  $We=4294$ ,  $J=0.253$ .

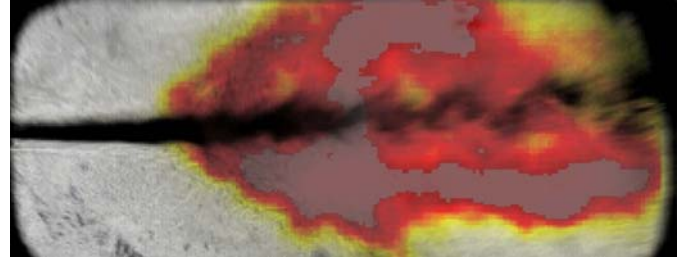


Figure 13: LOX/CH<sub>4</sub> spray and flame visualization for  $We=12582$ ,  $J=0.099$ .

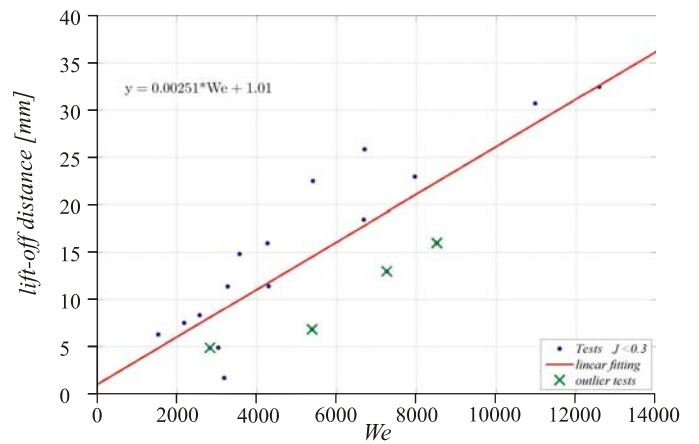


Figure 14: Lift-off distance of the LOX/CH<sub>4</sub> spray flame for tests with  $J < 0.3$ .

Finally it has been investigated whether the role of the non-dimensional group  $\Psi = h_s / \delta_f$  with respect to flame stabilization observed in numerical investigations by Juniper and Candel [18] is confirmed by our experiments. In their work they found for  $\Psi > 1$  flames stabilized at the step whereas for  $\Psi < 1$  unstable solutions have been obtained. In order to compare  $\Psi$  for H<sub>2</sub>/O<sub>2</sub> and CH<sub>4</sub>/O<sub>2</sub> the flame thickness  $\delta_f$  has to be evaluated for both propellant pairs. The chemical time scale for H<sub>2</sub>/O<sub>2</sub> is less than for CH<sub>4</sub>/O<sub>2</sub> and the species diffusivity for H<sub>2</sub>/O<sub>2</sub> is greater than for CH<sub>4</sub>/O<sub>2</sub>. Thus these opposite trends balance each other in determining the flame thickness using  $\delta_f = 1 / \sqrt{\tau_c \mathcal{D}}$  (see eq. (3)). To evaluate the value of  $\Psi$  quantitatively the flame thickness  $\delta_f$  has been estimated using

$$\delta_f = \frac{\mathcal{D}}{u_0}$$

where  $u_0$  is the laminar premixed burning velocity. Species diffusivities have been determined for STP conditions. With these assumptions a flame front thickness of  $\delta_f = 12 \cdot 10^{-6}$  m for

$H_2/O_2$  and  $\delta_f=5.5 \cdot 10^{-6}$  m for  $CH_4/O_2$  is been obtained. With the LOX post thickness of  $h_s=0.4$  mm this results in  $\Psi_{H_2}=33$  for  $H_2/O_2$  and  $\Psi_{CH_4}=72$  for  $CH_4/O_2$ . Both values are thus clearly in favour of an attached flame with respect of the arguments given in [18]. Nevertheless detached flames have been found in our experiments for  $CH_4/O_2$ . M. Micci did a similar analysis assuming  $p_c=1$  MPa and  $T=1000$  K [20] and obtained  $\Psi_{H_2}=70$  and  $\Psi_{CH_4}=87$ . Again both values would favour attached flames. For both estimations it is  $\Psi_{H_2} < \Psi_{CH_4}$  indicating that methane flames should be stabilized more easily at the injector than hydrogen flames. The contrary has been observed,  $H_2/O_2$  flames have been found always attached and  $CH_4/O_2$  flames have been found rather always detached. A deeper analysis seems necessary to explain the situation.

## Summary and Conclusions

Characteristics of reactive cryogenic sprays at hot fire conditions for the two propellant pairs  $H_2/O_2$  and  $CH_4/O_2$  have shown similar trends with respect to the effect of momentum flux ratio  $J$  and  $We$ . Increasing  $J$  is resulting in an earlier onset of jet disintegration, increasing Weber number is promoting disintegration into smaller ligaments and droplets at smaller distances downstream from the injector. However at similar injection conditions in terms of  $J$  and  $We$  the spray patterns for the two propellant pairs are significantly different. Due to the interaction of combustion with the liquid jet disintegration the LOX atomization process is also sensitive to the fuel type. The intact core length for LOX/ $CH_4$  sprays has been found to scale with  $J^n$ . An observed dependence of the intact core length from the LOX post thickness could be explained by an effect of the  $We$ -number.

At our experimental conditions LOX/ $H_2$  flames have always been found attached to the injector whereas rather all LOX/ $CH_4$  flames were detached. For momentum flux ratios  $J < 0.3$  a linear dependence of the flame lift-off distance for LOX/ $CH_4$  flames has been observed. The non-dimensional group  $\Psi$ , the ratio of LOX post thickness and flame thickness, does not explain the observed different stabilization behaviour for LOX/ $H_2$  and LOX/ $CH_4$  flames.

At the pressure levels that can be realized with the micro combustor at the M3.1 test bench the range of  $J$  values is limited. Due to this there have been only few tests with  $J > 2$ . More data would be therefore desirable especially at higher pressure to extend the analysis to  $J$ -values representative for propellant injection in rocket combustors.

## ACKNOWLEDGEMENT

The authors gratefully acknowledge the contribution of Mike Micci to the discussion of flame stabilization of LOX/ $H_2$  and LOX/ $CH_4$  spray flames.

## NOMENCLATURE

Symbol	Quantity	SI Unit
$d$	diameter	m
$\mathcal{D}$	species diffusivity	$m^2/s$
$h_s$	step height	m
$J$	momentum flux ratio	-
$L$	liquid core length	m
$p_c$	chamber pressure	MPa

$u$	velocity	m/s
$We$	Weber number	-
$\rho$	density	$kg/m^3$
$\sigma$	surface tension	$N/m^2$
$\tau_c$	chemical time scale	s

## REFERENCES

- [1] Arnold R., Suslov D., Haidn O.J., "Experimental Investigation of Film Cooling with Tangential Slot Injection in a LOX/ $CH_4$  – Subscale Rocket Combustion Chamber", ISTS, Japan, 2008
- [2] Slavinskaya, N.A., Haidn, O.J., "Reduced Chemical Model for High Pressure Methane Combustion with PAH Formation", AIAA-2008-1012, Reno, 2008
- [3] Yang B., Cuoco F., Oschwald M., "Atomization and Flames in LOX/ $H_2$ - and LOX/ $CH_4$  spray combustion", *Journal of Propulsion and Power*, Vol. 23, No. 4, 2007
- [4] Pauly C., Sender, J., Oschwald M., "Ignition of a Gaseous Methane/Oxygen Coaxial Jet", 2nd European Conference for Aerospace Sciences (EUCASS), Brussels, 2007
- [5] Ledoux M., Caré I., Glogowski M., Vingert L., Gicquel P., "Atomization of Coaxial Injectors", *2nd Int. Symposium on Liquid Rocket Propulsion*, Châtillon, France, 1995
- [6] C. Engelbert, Y. Hardalupas, J. H. Whitelaw, "Breakup Phenomena in Coaxial Airblast Atomizer", *Proc. R. Soc. Lond. A* (1995) 451, 189-229, 1995
- [7] Villiermaux E., "Mixing and Spray Formation in Coaxial Jets", *Journal of Propulsion and Power*, Vol. 14, No. 5, 1998.
- [8] Hardalupas Y., Whitelaw J.H., "Characteristics of Sprays Produced by Coaxial Airblast Atomizers", *Journal of Propulsion and Power*, Vol. 10, No. 4, 1994.
- [9] Porcheron E., Carreau J.L., Prevost L., Le Visage D., Roger F., "Effect of Injection Gas Density on Coaxial Liquid Jet Atomization", *Atomization and Sprays*, vol. 12, 2002.
- [10] Vingert L., Gicquel P., Lourme D., Ménoret L., "Coaxial Injector Atomization", *Liquid Rocket Combustion Instability in Progress in Astronautics and Aeronautics*, V. Yang, Anderson W. (Eds.), AIAA, New York, Vol. 169, 1994, 145-189
- [11] Farago Z., Chigier N., "Morphological Classification of Disintegration of Round Liquid Jets", *Atomization and Sprays*, Vol. 2, No. 2, 1992, pp. 137-153
- [12] Lasheras J.C., Villiermaux E., Hopfinger E.J., "Break-up and atomization of a round water jet by a high-speed annular air jet", *Journal of Fluid Mechanics*, Vol. 357, pp. 351-379, 1998
- [13] Davis, D. W., "On the behavior of a Shear-coaxial Jet, Spanning Sub- to Super-critical Pressures, With and Without an Externally Imposed Transverse Acoustic Field," Ph.D. Thesis, Dept. of Mech. And Nuc. Eng., The Pennsylvania State University, 2006.
- [14] Woodward, R. D., Pal, S., Farhangi, S., Santoro, R. J., "LOX/ $GH_2$  Shear Coaxial Injector Atomization Studies at Large Momentum Flux Ratios," *AIAA 2006-5203*, 42<sup>nd</sup> AIAA/ASME/SAE/ASEE Joint Propulsion Conf. & Exhibit, CA, 2006
- [15] Rahman S.A., Santoro R.J., "A Review of Coaxial Gas/Liquid Spray Experiments and Correlations", *AIAA 94-2772*, 30th Joint Propulsion Conference, Indianapolis, 1994

- [16] Smith J.J., Bechle M., Suslov D., Oswald M., Haidn O., Schneider G., "Steady-State High Pressure LO<sub>x</sub>/H<sub>2</sub> Rocket Engine Combustion", *1st European Conference for Aerospace Sciences (EUCASS)*, July 4-7, 2005, Moscow, Russia
- [17] Oswald M., Schik A., Klar M., Mayer W., "Investigation of coaxial LN<sub>2</sub>/GH<sub>2</sub>-injection at supercritical pressure by spontaneous Raman scattering", *AIAA 99-2887*, 35th Joint Propulsion Conference and Exhibit, Los Angeles, Ca, 1999
- [18] Juniper M., Candel S., "Edge Diffusion Flame Stabilization Behind a Step over a Liquid Reactant", *Journal of Propulsion and Power*, Vol. 19, No. 3, 2003, pp. 332-341
- [19] Chehroudi B., Talley D., Mayer W., Branam R., Smith J., Schik A., Oswald M., "Understanding injection into high pressure supercritical environments", *5th International Conference on Liquid Rocket Propellant*, Chattanooga, 2003
- [20] Micci M.M., private communication